

Ji Soo Choi
Myeong-Jin Kim
Jin-Young Choi
Mi-Suk Park
Joon Seok Lim
Ki Whang Kim

Diffusion-weighted MR imaging of liver on 3.0-Tesla system: effect of intravenous administration of gadoxetic acid disodium

Received: 3 July 2009
Revised: 9 September 2009
Accepted: 10 October 2009
Published online: 14 November 2009
© European Society of Radiology 2009

J. S. Choi · M.-J. Kim · J.-Y. Choi ·
M.-S. Park · J. S. Lim · K. W. Kim
Department of Radiology, Severance
Hospital and Research Institute of
Radiological Science, Yonsei
University College of Medicine,
Seoul, Korea

M.-J. Kim
Institute of Gastroenterology and Brain
Korea 21 Project, Yonsei University
College of Medicine,
Seoul, Korea

M.-J. Kim (✉)
Department of Diagnostic Radiology,
Yonsei University College of Medicine,
134 Shinchon-Dong, Seodaemun-gu,
Seoul, 120-752, Korea
e-mail: kimmex@yuhs.ac
Tel.: +82-2-22287400
Fax: +82-2-3933035

Abstract Objective: To determine whether intravenous administration of gadoxetic acid disodium (Gd-EOB-DTPA) affects lesion conspicuity and apparent diffusion coefficient (ADCs) in diffusion-weighted imaging (DWI) for hepatic magnetic resonance imaging (MRI) at 3.0 T. **Methods:** Thirty-four patients with 50 focal hepatic lesions (18 hepatocellular carcinomas, 12 metastases, 1 cholangiocarcinoma, 7 haemangiomas, 12 cysts) underwent DWI at 3.0 T before and after administration of Gd-EOB-DTPA. Non-breath-hold DWI was performed with b values of 0, 200, 400 and 800 s/mm². Signal-to-noise ratio (SNR) and contrast-to-noise ratio (CNR) of each lesion, and ADCs of the liver and lesion were calculated for unenhanced and enhanced images. Statistical differences between unenhanced and enhanced data were assessed. **Results:** SNRs and ADCs

of the liver on enhanced images were significantly lower than on unenhanced images. On DW images at $b = 200$ s/mm², CNRs of malignant and overall lesions were significantly higher on enhanced than on unenhanced images. CNRs of focal lesions tended to be higher, especially in malignant lesions, on DW images at $b = 0$ and 400 s/mm², but without reaching statistical significance. ADCs of focal hepatic lesions were not significantly different before and after administration of contrast agent. **Conclusion:** DWI after Gd-EOB-DTPA administration can be used as a substitute for unenhanced DWI at 3.0 T without compromising CNR and ADC of focal hepatic lesions.

Keywords Diffusion-weighted imaging · Magnetic resonance imaging · 3.0 T · Gadoxetic acid disodium · Hepatic lesion

Introduction

Diffusion, or Brownian motion, is thermally induced motion of water molecules in the body [1, 2]. The motion of water molecules is restricted in tissues with increased cellularity and numerous intact cell membranes [3, 4]. Diffusion-weighted imaging (DWI) using diffusion-sensitising gradient pulses can be used to detect and quantify the molecular diffusion in the body by means of apparent diffusion coefficient (ADC) measurement [1, 2].

With the advent of echo-planar imaging, diffusion-weighted imaging (DWI) is increasingly being used for

the evaluation of focal hepatic lesions [5–8]. DWI can be applied to tumour detection by depicting subtle signal attenuation on images obtained at different b values [9, 10]. DWI can also be used as a quantitative tool for lesion characterisation via ADC measurements [6, 9, 11].

In liver magnetic resonance imaging (MRI), DWI may be added to existing protocols and is usually performed before administration of intravenous contrast agents. However, under certain circumstances, DWI after administration of contrast material may be desirable if it can achieve equivalent results. For example, when liver MRI is performed using gadoxetic acid disodium (Gd-EOB-DTPA; gadolinium-

ethoxybenzyl-diethylene-triamine-pentaacetic-acid), a paramagnetic contrast agent with properties of both extracellular and hepatobiliary agents, acquisition of hepatobiliary phase images at 10–20 min after injection may improve diagnostic accuracy in the detection and characterisation of focal liver lesions in addition to the dynamic imaging [12–14]. Thus, it can save time to perform DWI during the interval between early dynamic and hepatobiliary imaging.

Although a previous study demonstrated the feasibility of enhanced DWI in liver MRI using gadopentetate dimeglumine (Gd-DTPA) [15], the effects of Gd-EOB-DTPA on DWI or the measured ADC have not been examined. Unlike extracellular contrast agents such as Gd-DTPA, approximately 50% of the injected dose of Gd-EOB-DTPA is specifically taken up into hepatocytes [12, 14, 16]. Moreover, Gd-EOB-DTPA shows almost two-fold higher T1 and T2 relaxivities compared with conventional gadolinium chelates on both 1.5-T and 3.0-T MR systems [17]. Therefore, Gd-EOB-DTPA has a higher potential to alter the ADCs and signal intensities of DW images by further increasing magnetic susceptibility and T2 shortening, compared with Gd-DTPA.

The aim of this study was to assess whether administration of Gd-EOB-DTPA significantly affects lesion conspicuity and ADC values on DWI for hepatic MRI on a 3.0-T system.

Materials and methods

Patient sample

From April to June 2008, 34 patients (28 men and 6 women; age range 37–78 years, mean 62.5 years) underwent Gd-EOB-DTPA-enhanced MRI with DWI before and after injection of contrast agent at Yonsei University Severance Hospital. The MRI examinations were performed because these patients had focal hepatic lesions that were inconclusive on previous sonography or computed tomography (CT). This study was approved by the institutional review board at the hospital, and informed consent was waived.

A total of 50 focal hepatic lesions in 34 patients were assessed by DWI. There were 18 hepatocellular carcinomas (HCC) in 11 patients, 12 metastases in 11 patients, 1 cholangiocarcinoma in 1 patient, 7 haemangiomas in 7 patients, and 12 cysts in 5 patients. Among the nine patients with multiple lesions, only one patient had more than one type of lesion (one HCC and one haemangioma). Liver metastases arose from the following primary tumours: colorectal carcinoma (10 lesions in nine patients) and gastric carcinoma (2 lesions in two patients). The diameters of the lesions ranged from 1 to 8.1 cm (mean 2.6 cm). Specifically, the diameters of the HCCs ranged from 1 to 4.3 cm (mean 2.6 cm), diameters of the metastases ranged from 1 to 8.1 cm (mean 3.3 cm), the

diameter of the cholangiocarcinoma was 2.8 cm, diameters of the haemangiomas ranged from 1 to 3.8 cm (mean 2.1 cm), and diameters of the cysts ranged from 1 to 4.4 cm (mean 2.1 cm).

Diagnoses were confirmed using the following parameters. The imaging parameters included only typical findings of contrast-enhanced MRI or CT, or unenhanced sonography in this study. A diagnosis of HCC was based on typical MRI findings described in previous literature [18–21] including intense enhancement in the arterial phase and contrast medium washout in the delay phase during gadolinium-enhanced imaging, mosaic pattern, tumour capsule and extracapsular extension with satellite nodules in combination with the progression of the disease presented on follow-up CT or MR images, and confirmed by surgery (5 lesions in three patients) or the elevation of serum α -fetoprotein levels in patients (13 lesions in eight patients). Liver metastasis was diagnosed on the basis of the histological findings of the primary tumour and rapid progression as depicted on serial follow-up images (five lesions in four patients) or by surgery (seven lesions in seven patients). A cholangiocarcinoma was diagnosed by surgery. In cases of haemangioma, diagnosis was based on the typical findings on MRI including nodular or globular enhancement with a gradual filling-in pattern on dynamic MRI, very high signal intensity on both moderate and heavily T2-weighted images, and the lack of growth on CT or MR images during a follow-up period of at least 6 months (six lesions in six patients) or on biopsy (one lesion in one patient). Cysts were diagnosed on the basis of their typical appearance on non-enhanced T1- and T2-weighted MRIs (markedly low signal intensity on T1-weighted images and very high signal intensity on both moderate and heavily T2-weighted images and the absence of contrast enhancement), and the findings were correlated with either ultrasound or CT findings.

MRI

All patients were examined with a 3.0-T MR system (MAGNETOM Trio a Tim; Syngo MR B15; Siemens Medical Solutions, Erlangen, Germany). All images were obtained in the transverse plane using a single dedicated body phased array coil anterior and spine array coils posterior (Fig. 1).

Routine liver MRIs were acquired using the following sequences: two breath-hold T1-weighted spoiled GRE in-phase sequence [repetition time (TR)/effective echo time (TE), 140/1.22 ms] and out-of-phase (150/2.5) with a flip angle of 65°, one signal acquired, a matrix of 256×192, 7 mm slice thickness and a 0.7 mm gap; a navigator-triggered T2-weighted turbo spin-echo (TSE) sequence with TR range of 3,300–4,900 and TE 73 ms, echo train

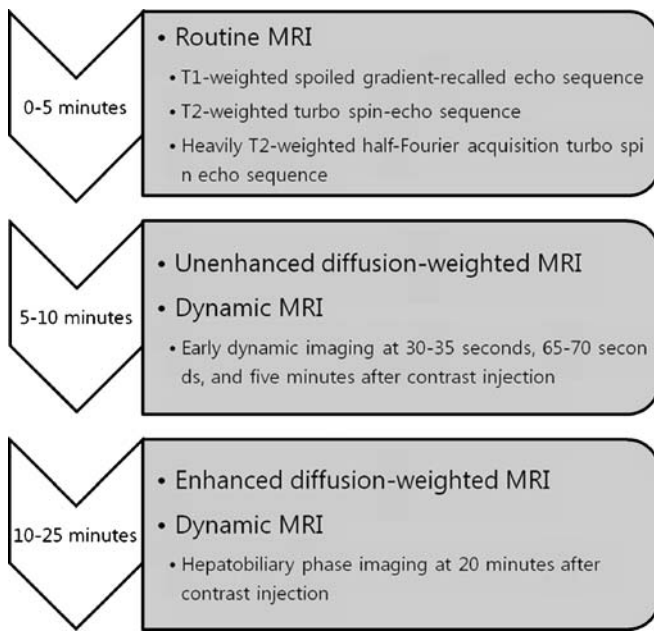


Fig. 1 Scanning protocols of routine MRI, unenhanced and enhanced diffusion-weighted imaging (DWI)

length of 14, one signal acquired, a matrix of 320×179 , superior and inferior spatial presaturation and chemical fat saturation, 4 mm slice thickness and a 1 mm gap; a breath-hold, heavily T2-weighted half-Fourier acquisition turbo spin echo (HASTE) with TE of 150 ms, a matrix of 320×179 , 4 mm slice thickness and a 1 mm gap.

For dynamic MRI, Gd-EOB-DTPA (Primovist, Bayer Schering; 0.025 mmol/kg) was injected as a rapid bolus and immediately followed by a 30 ml saline flush through a power injector at a rate of 2 ml/s. A three-dimensional (3D) spoiled GRE sequence with chemical selective fat suppression was performed before injection of intravenous contrast agent. Contrast-enhanced images were obtained at 30–35 s, 65–70 s, and 5 min after the injection. Hepatobiliary phase images were obtained 20 min after contrast injection [12–14]. The MR parameters included TR/TE 3.3/1.16, a flip angle of 13° , a 256×192 matrix, one signal acquired, and 2.5 mm slice thickness with a zero intersection gap.

Diffusion-weighted MRI

Two navigator-triggered DWI sequences were performed with the single-shot echo planar imaging with motion-probing gradients in three directions, before and after contrast agent injection. For monitoring respiration, the prospective acquisition correction (PACE) technique, in which the diaphragmatic position is assessed periodically by navigator echoes, was implemented. Enhanced DWI was performed at approximately 7 min after injection of the contrast agent. Unenhanced and enhanced DWI were

acquired using the same parameters as follows: b values of 0, 200, 400, and 800 s/mm^2 , TR/TE 1,400/74, two signals acquired, a matrix of 192×153 , 8 mm slice thickness, and an acquisition time of 2 min. The ADCs for each DWI were automatically calculated by the MR system and displayed as corresponding ADC maps.

Image analysis

Two abdominal radiologists (M.J.K and J.Y.C) with 17 and 8 years of experience, who were blinded to the clinical details, evaluated all MR images in consensus. The focal hepatic lesions were identified on the T1- and T2-weighted and dynamic images. The signal intensities (SI), size, number and location of lesions, as well as the enhancement pattern, were assessed in each case on the MR images. Because of the limited resolution of DWI, only lesions more than 1 cm in diameter were included for the quantitative analysis of this study.

Quantitative analysis was performed by a fourth-year radiology resident (C.J.S). Regions of interest (ROIs) were drawn in the focal lesion, hepatic parenchyma, and background noise at a workstation (Centricity 2.0, GE Healthcare, U.S.A.) to measure SI on DW images at b values of 0 s/mm^2 . The area of the ROI in the focal lesion was set to measure the homogeneous area of the lesion while avoiding areas of necrosis, haemorrhage or fibrosis and to maintain an area of at least 20 mm^2 . The ROI of the liver was placed in the posterior right hepatic lobe, specifically at the level of the main portal vein and its right branches, while excluding vessels and artefacts. The SI of the background noise was measured in the ROI that was just ventral to the liver and outside the body along the phase encoding direction. The areas of the ROI in the liver and background were maintained at larger than 100 and 500 mm^2 , respectively. To ensure identical placement of the ROIs on the DW images at b values of 0, 200, 400 and 800 s/mm^2 , ROIs were manually and carefully positioned to be in the same region of DW images at different b values. The lesion-to-liver contrast-to-noise ratio (CNR) was calculated using the following equation:

$$CNR = (SI_{lesion} - SI_{liver}) / SD_{noise}$$

where SI_{lesion} is the SI of the lesion, SI_{liver} is the SI of the liver, and SD_{noise} is the standard deviation of the background noise. The signal-to-noise ratio (SNR) was calculated from the following equation:

$$SNR = SI_{liver \text{ or } lesion} / SD_{noise}$$

The mean SNR and CNR for unenhanced and enhanced DWI were also calculated.

ADC measurements were performed by placing ROIs on focal hepatic lesions and hepatic parenchyma on ADC maps. For identical placement of ROI on DW images and ADC maps, where the ADC values were simultaneously displayed on the workstation, ROIs were carefully positioned in the same region on corresponding ADC maps. The mean ADCs of liver and focal lesions were calculated from unenhanced and enhanced DWI.

Statistical analysis

The paired *t*-test was used for comparison of the SNR, CNR and ADC values between unenhanced and enhanced DWI. The Kruskal-Wallis test was performed in order to assess statistically significant differences among the mean ADC values of the different types of focal hepatic lesions, and the Mann-Whitney test was

Table 1 Signal-to-noise ratios (SNRs) of the liver and focal hepatic lesions on DWI

	Number of patients	Number of lesions	Unenhanced	Enhanced	<i>p</i> Value
<i>b</i> = 0 s/mm ²					
Liver	34		21.13±8.05	18.45±7.07	<0.001*
HCC	11	18	47.56±23.40	46.13±19.30	0.578
Metastatic disease	11	12	85.53±36.64	87.66±42.96	0.591
Haemangiomas	7	7	111.47±38.82	104.94±37.05	0.449
Cysts	5	12	112.02±56.96	114.19±56.43	0.799
Cholangiocarcinoma	1	1	174.94	205.17	None
Malignant lesions	23	31	66.37±39.43	67.33±44.23	0.677
Benign lesions	12	19	111.82±49.85	110.78±49.24	0.864
All focal lesions	34	50	83.64±48.59	83.84±50.42	0.939
<i>b</i> = 200 s/mm ²					
Liver	34		23.67±12.04	19.62±9.63	<0.001*
HCC	11	18	53.26±22.94	55.75±33.25	0.482
Metastatic disease	11	12	104.74 ±58.44	116.23±64.03	0.170
Haemangiomas	7	7	103.48±49.41	100.95±42.78	0.879
Cysts	5	12	100.51 ± 40.42	101.50±49.81	0.926
Cholangiocarcinoma	1	1	95.44	122.27	None
Malignant lesions	23	31	74.55±46.92	81.31±55.36	0.104
Benign lesions	12	19	99.22±42.31	101.53±47.57	0.789
All focal lesions	34	50	83.92±46.39	88.99±52.97	0.204
<i>b</i> = 400 s/mm ²					
Liver	34		17.50±7.00	14.79±6.64	<0.001*
HCC	11	18	40.42±18.49	41.76±29.33	0.716
Metastatic disease	11	12	84.90±44.31	90.03±48.67	0.483
Haemangiomas	7	7	70.83±46.11	64.18±28.24	0.483
Cysts	5	12	72.71±45.08	77.07±53.17	0.304
Cholangiocarcinoma	1	1	81.69	98.84	None
Malignant lesions	23	31	58.97±37.50	62.29±44.29	0.340
Benign lesions	12	19	72.02±44.18	72.33±45.11	0.956
All focal lesions	34	50	63.93±40.23	66.10±44.41	0.464
<i>b</i> = 800 s/mm ²					
Liver	34		13.20±4.78	10.95±3.62	0.001*
HCC	11	18	35.90±15.13	30.29±19.78	0.083
Metastatic disease	11	12	60.58±39.56	60.12±25.36	0.944
Haemangiomas	7	7	45.81±26.34	32.57±18.00	0.043*
Cysts	5	12	22.70±12.69	23.43±16.55	0.798
Cholangiocarcinoma	1	1	57.09	70.18	None
Malignant lesions	23	31	46.14±29.22	43.12±26.38	0.338
Benign lesions	12	19	31.21±21.46	26.80±17.20	0.154
All focal lesions	34	50	40.47±27.30	36.92±24.47	0.115

**p* Value <0.05

Data represent means ± SD

used to compare the mean ADC values of each type of lesion and two groups of lesions on the two DWI sequences. All focal hepatic lesions were classified into a malignant group (18 HCCs, 12 metastases and 1 cholangiocarcinoma) and a benign group (7 haemangiomas and 12 cysts).

For all tests, a p value less than 0.05 was considered to indicate a statistically significant difference. Statistical analyses were performed with version 9 of Medcalc (Medcalc Software, Belgium).

Results

The SNRs of the liver and focal hepatic lesions on DW images are shown in Table 1. Liver SNRs were significantly higher on unenhanced than on enhanced DWI at all b values. There was an approximately 16% decrease in mean SNR on enhanced DW images. The mean liver SNR was highest on DW images with a b value of 200 s/mm² on both unenhanced and enhanced DWI. The SNRs of overall lesions and of each type of lesion were not significantly different on the unenhanced and enhanced DWI. There was a tendency for SNRs of focal hepatic

Table 2 Contrast-to-noise ratios (CNRs) of the focal hepatic lesions on DWI

	Number of patients	Number of lesions	Unenhanced	Enhanced	p Value
$b = 0 \text{ s/mm}^2$					
HCC	11	18	28.69±21.76	30.71±17.70	0.376
Metastatic disease	11	12	66.68±33.62	71.26±39.70	0.245
Haemangiomas	7	7	85.40±38.36	86.51±41.61	0.659
Cysts	5	12	96.60±56.00	100.59±55.72	0.639
Cholangiocarcinoma	1	1	146.17	184.30	None
Malignant lesions	23	31	47.19±36.97	51.36±41.93	0.070
Benign lesions	12	19	92.47±49.38	93.59±48.94	0.853
All focal lesions	34	50	64.39±47.17	67.41±48.84	0.255
$b = 200 \text{ s/mm}^2$					
HCC	11	18	33.21±23.22	38.70±27.51	0.008*
Metastatic disease	11	12	84.50±55.82	98.18±61.74	0.112
Haemangiomas	7	7	72.72±42.79	75.40±37.97	0.864
Cysts	5	12	84.87±40.47	87.78±49.66	0.781
Cholangiocarcinoma	1	1	77.65	106.62	None
Malignant lesions	23	31	54.50±45.83	63.92±52.33	0.008*
Benign lesions	12	19	78.05±40.01	83.46±46.51	0.520
All focal lesions	34	50	63.45±44.80	71.35±50.65	0.038*
$b = 400 \text{ s/mm}^2$					
HCC	11	18	25.53±17.65	29.77±27.62	0.187
Metastatic disease	11	12	67.79±41.87	75.51±46.85	0.187
Haemangiomas	7	7	50.19±46.34	46.15±25.31	0.774
Cysts	5	12	56.73±42.42	61.23±49.91	0.257
Cholangiocarcinoma	1	1	67.66	87.97	None
Malignant lesions	23	31	43.25±35.61	49.36±42.32	0.060
Benign lesions	12	19	54.32±42.73	55.67±42.33	0.803
All focal lesions	34	50	47.45±38.43	51.76±42.00	0.130
$b = 800 \text{ s/mm}^2$					
HCC	11	18	21.50±16.35	20.72±19.11	0.771
Metastatic disease	11	12	48.40±39.55	49.14±25.39	0.908
Haemangiomas	7	7	31.77±28.21	22.01±16.89	0.093
Cysts	5	12	11.33±11.87	12.89±14.35	0.559
Cholangiocarcinoma	1	1	43.87	59.87	None
Malignant lesions	23	31	32.63±30.05	32.98±25.73	0.902
Benign lesions	12	19	18.86±21.30	16.25±15.53	0.343
All focal lesions	34	50	27.40±27.66	26.63±23.69	0.704

* p Value <0.05

Data represent means ± SD

lesions to decrease with increasing b values on both unenhanced and enhanced DWI. The SNRs of malignant lesions, however, were highest on DW images at a b value of 200 s/mm^2 on both unenhanced and enhanced DWI. There was also a tendency for SNRs of malignant lesions to be increased on enhanced DWI at b values of 200 and 400 s/mm^2 , but this difference did not reach statistical significance.

Table 2 shows CNRs of focal hepatic lesions on unenhanced and enhanced DW images. On DW images at a b value of 200 s/mm^2 , the CNRs of malignant and overall lesions were significantly higher on enhanced than on unenhanced images. Also, there was a trend towards increasing CNRs of focal lesions on DW images at b values of 0 and 400 s/mm^2 without reaching statistical significance, especially in malignant lesions. Additionally, there was no significant difference in the CNRs between unenhanced and enhanced DWI at a b value of 800 s/mm^2 .

The unenhanced and enhanced ADC values of the liver and focal hepatic lesions are shown in Table 3. The ADC values of liver were significantly lower on enhanced than on unenhanced DW images. Liver showed an approximately 5% decrease in mean ADC on enhanced images. However, there was no significant difference in the ADC values between unenhanced and enhanced DWI sequences for overall lesions or for each type of lesion (Fig. 2). Box plots of the ADC values of each type of lesion on unenhanced and enhanced DWI (Fig. 3) show that ADC values of metastases overlapped with ADC values of HCCs and the cholangiocarcinoma on both unenhanced and enhanced DWI sequences. ADC values of haemangiomas were lower than those of cysts, but higher than those of the malignant group (HCCs, metastases and cholangiocarcinoma) on the two sequences. The ADC values of the malignant group were significantly lower than those of the benign group (Fig. 4) on both unenhanced and enhanced DWI sequences.

Discussion

This study showed that the SNR and ADC of liver were significantly lower on enhanced than on unenhanced DW images, although a previous study using Gd-DTPA did not show significant decreases in SNR and ADC of liver after administration of the contrast agent [15]. These results may be explained in two ways. First, as Gd-EOB-DTPA has both hepatobiliary and extracellular properties, it can be taken up selectively by functioning hepatocytes and excreted through the biliary tract as early as 5–10 min after injection [12–14, 22]. Because enhanced DWI in the current study was acquired between 7 and 10 min after administration of the contrast agent, Gd-EOB-DTPA would have already been taken up into the hepatocytes of the liver at the time of acquisition of this sequence. Consequently, the decrease in liver SNR on enhanced DWI may be caused by T2 shortening of highly concentrated Gd-EOB-DTPA in the liver. Second, the higher T2 relaxivity of Gd-EOB-DTPA may also cause decreased values of ADC in the liver. Compared with Gd-DTPA, the T2 relaxivity of Gd-EOB-DTPA has been reported to be two-fold higher and can be even higher with the use of 3.0-T systems than with 1.5-T systems [17].

The SNRs and ADC values of focal hepatic lesions were comparable on unenhanced and enhanced images at all b values. This result indicates that the administration of Gd-EOB-DTPA does not affect the signal intensity or ADC values of focal liver lesions that are usually devoid of the contrast agent. Although the SNRs of liver were significantly lower on enhanced images at all four b values while the SNRs of focal liver lesions showed no significant differences, the CNRs of focal liver lesions were comparable on unenhanced and enhanced images, except at a b value of 200 s/mm^2 , at which the CNRs of malignant lesions, mostly HCC, were significantly higher compared with unenhanced images. This result can be explained by the considerably lower values of SI in liver than in focal liver lesions on both unenhanced and enhanced DW images.

Table 3 ADC values ($\times 10^{-3}$) of the liver and focal hepatic lesions

	Number of patients	Number of lesions	Unenhanced	Enhanced	p Value
Liver	34		1.26 \pm 0.15	1.20 \pm 0.17	0.010*
HCC	11	18	1.08 \pm 0.30	1.16 \pm 0.32	0.172
Metastatic disease	11	12	1.22 \pm 0.42	1.21 \pm 0.37	0.864
Haemangiomas	7	7	1.74 \pm 0.51	1.71 \pm 0.31	0.771
Cysts	5	12	3.15 \pm 0.26	3.14 \pm 0.28	0.897
Cholangiocarcinoma	1	1	1.028	0.956	None
Malignant lesions	23	31	1.13 \pm 0.35	1.17 \pm 0.33	0.299
Benign lesions	12	19	2.63 \pm 0.78	2.61 \pm 0.76	0.782
All focal lesions	34	50	1.70 \pm 0.92	1.72 \pm 0.88	0.567

* p Value <0.05

Data represent means \pm SD

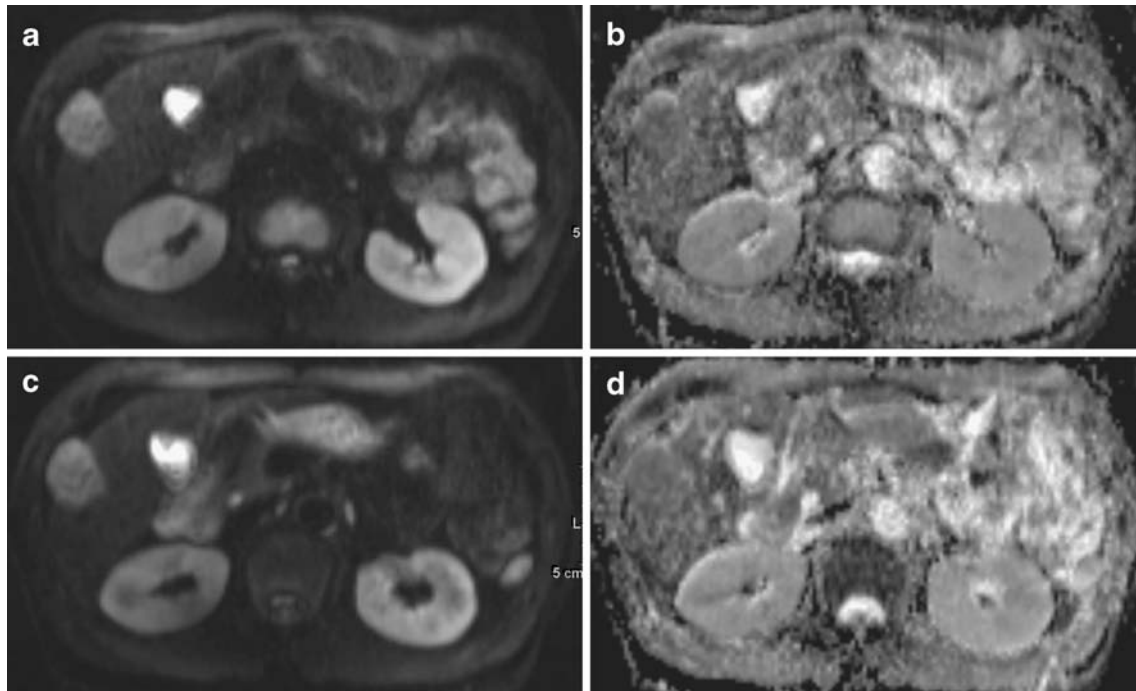


Fig. 2 A 47-year-old man with a hepatocellular carcinoma (HCC) and chronic hepatitis B virus. Transverse diffusion-weighted images (DWI) and apparent diffusion coefficient (ADC) maps of unenhanced (a and b respectively) and enhanced (c and d respectively) DWI sequences. The HCC shows hyperintensity on DWI and a low

ADC value. The liver signal is slightly lower on the enhanced than on the unenhanced images. However, the overall appearance of the liver, HCC and lesion conspicuity are not significantly different on the unenhanced and enhanced images

at all *b* values. The relatively small difference in SNR of liver did not significantly affect CNR in this study, especially at higher *b* values (400 and 800 s/mm²). On DW images at a *b* value of 200 s/mm², however, the

contributions of liver SI to CNR were relatively greater compared with DW images at higher *b* values. Hence, the CNR of focal hepatic lesions was significantly higher on enhanced images at *b* values of 200 s/mm². Although the

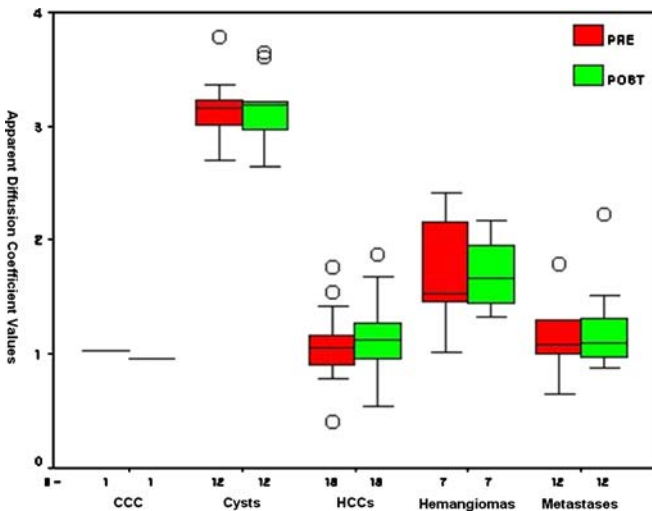


Fig. 3 Box plots of the ADC values ($\times 10^{-3}$) of each type of lesion. ADC values and their scatter are similar on unenhanced and enhanced DWI sequences. CCC Cholangiocarcinoma, HCCs hepatocellular carcinomas

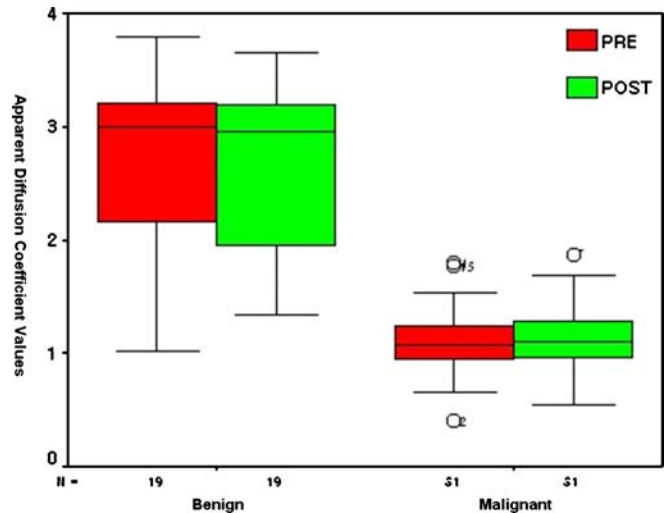


Fig. 4 Box plots of the ADC values ($\times 10^{-3}$) of malignant and benign lesions. ADC values and their scatter are not significantly different on the two sequences. Malignant includes hepatocellular carcinomas, metastases and cholangiocarcinoma; benign includes cysts and haemangiomas

CNRs were not significantly increased at higher b values, relative decreases in the SNR of liver on enhanced DWI may be helpful for improving lesion conspicuity.

For the evaluation of the Gd-EOB-DTPA effect on lesion characterisation, we compared ADC values of each type of lesion and two groups of lesions (malignant vs. benign) on unenhanced and enhanced DWI. The ADC values of each type of lesion were comparable on unenhanced and enhanced DWI sequences. Lesions of the malignant group showed significantly lower ADC values than those of the benign group on both unenhanced and enhanced DWI. These findings indicate that DWI obtained after dynamic imaging using Gd-EOB-DTPA can yield comparable results for lesion characterisation compared with unenhanced images.

A limitation of this study is that the slice locations of paired DWI sequences may not have been perfectly matched. Although we carefully excluded focal lesions with a possibility of misregistration between unenhanced and enhanced DWI, this condition may not have been completely avoided. Another limitation of the study is that the patient sample was heterogeneous, and the sample size

was relatively small. However, we believe that the intra-individual comparisons performed in our study should overcome these drawbacks. Finally, we have not compared these combined dynamic MRI and DWI with dynamic MRI without DWI for the ability to detect and characterise liver lesions because the purpose of this study was only to evaluate whether Gd-EOB-DTPA affects lesion conspicuity and ADC values in DWI for liver MRI. Therefore, further studies about the cost-benefit effects of this combined dynamic MRI and DWI for liver MRI using Gd-EOB-DTPA may be needed.

In conclusion, our results suggest that acquisition of DWI during the interval between dynamic MRI and hepatobiliary imaging can be effective and time-saving without compromising CNR and ADC values of focal hepatic lesions. Instead, low signal intensity of the liver on enhanced DWI may be useful for improving lesion conspicuity by increasing the CNR of focal hepatic lesions on the images taken at lower b values. The ADC values of the liver and focal liver lesions measured on enhanced DW images were comparable to those obtained on unenhanced images with regard to lesion characterisation.

References

1. Le Bihan D, Turner R, Douek P, Patronas N (1992) Diffusion MR imaging: clinical applications. *AJR Am J Roentgenol* 159(3):591–599
2. Koh DM, Collins DJ (2007) Diffusion-weighted MRI in the body: applications and challenges in oncology. *AJR Am J Roentgenol* 188:1622–1635
3. Lang P, Wendland MF, Saeed M et al (1998) Osteogenic sarcoma: noninvasive in vivo assessment of tumor necrosis with diffusion-weighted MR imaging. *Radiology* 206:227–235
4. Guo Y, Cai YQ, Cai ZL et al (2002) Differentiation of clinically benign and malignant breast lesions using diffusion-weighted imaging. *J Magn Reson Imaging* 16:172–178
5. Okada Y, Ohtomo K, Kiryu S, Sasaki Y (1998) Breath-hold T2-weighted MRI of hepatic tumors: value of echo planar imaging with diffusion-sensitizing gradient. *J Comput Assist Tomogr* 22:364–371
6. Koh DM, Scurr E, Collins DJ et al (2006) Colorectal hepatic metastases: quantitative measurements using single-shot echo-planar diffusion-weighted MR imaging. *Eur Radiol* 16:1898–1905
7. Ichikawa T, Haradome H, Hachiya J, Nitatori T, Araki T (1998) Diffusion-weighted MR imaging with a single-shot echoplanar sequence: detection and characterization of focal hepatic lesions. *AJR Am J Roentgenol* 170:397–402
8. Butts K, Riederer SJ, Ehman RL, Felmlee JP, Grimm RC (1993) Echoplanar imaging of the liver with a standard MR imaging system. *Radiology* 189:259–264
9. Nasu K, Kuroki Y, Nawano S et al (2006) Hepatic metastases: diffusion-weighted sensitivity-encoding versus SPIO-enhanced MR imaging. *Radiology* 239:122–130
10. Moteki T, Sekine T (2004) Echo planar MR imaging of the liver: comparison of images with and without motion probing gradients. *J Magn Reson Imaging* 19:82–90
11. Bruegel M, Holzapfel K, Gaa J et al (2008) Characterization of focal liver lesions by ADC measurements using a respiratory triggered diffusion-weighted single-shot echo-planar MR imaging technique. *Eur Radiol* 18:477–485
12. Zech CJ, Herrmann KA, Reiser MF, Schoenberg SO (2007) MR imaging in patients with suspected liver metastases: value of liver-specific contrast agent Gd-EOB-DTPA. *Magn Reson Med Sci* 6:43–52
13. Reimer P, Schneider G, Schima W (2004) Hepatobiliary contrast agents for contrast-enhanced MRI of the liver: properties, clinical development and applications. *Eur Radiol* 14:559–578
14. Hamm B, Staks T, Muhler A et al (1995) Phase I clinical evaluation of Gd-EOB-DTPA as a hepatobiliary MR contrast agent: safety, pharmacokinetics, and MR imaging. *Radiology* 195:785–792
15. Chiu FY, Jao JC, Chen CY et al (2005) Effect of intravenous gadolinium-DTPA on diffusion-weighted magnetic resonance images for evaluation of focal hepatic lesions. *J Comput Assist Tomogr* 29:176–180
16. Reimer P, Rummeny EJ, Shamsi K et al (1996) Phase II clinical evaluation of Gd-EOB-DTPA: dose, safety aspects, and pulse sequence. *Radiology* 199:177–183
17. Rohrer M, Bauer H, Mintorovitch J, Requardt M, Weinmann HJ (2005) Comparison of magnetic properties of MRI contrast media solutions at different magnetic field strengths. *Invest Radiol* 40:715–724
18. Yu SC, Yeung DT, So NM (2004) Imaging features of hepatocellular carcinoma. *Clin Radiol* 59:145–156

19. Hussain SM, Zondervan PE, IJzermans JNM, Schalm SW, de Man RA, Krestin GP (2002) Benign versus malignant hepatic nodules: MR imaging findings with pathologic correlation. *Radiographics* 22:1023–1036; discussion 1037–1029
20. Hussain SM, Semelka RC, Mitchell DG (2002) MR imaging of hepatocellular carcinoma. *Magn Reson Imaging Clin N Am* 10:31–52
21. Elsayes KM, Narra VR, Yin Y, Mukundan G, Lammler M, Brown JJ (2005) Focal hepatic lesions: diagnostic value of enhancement pattern approach with contrast-enhanced 3D gradient-echo MR imaging. *Radiographics* 25:1299–1320
22. Bollow M, Taupitz M, Hamm B, Staks T, Wolf KJ, Weinmann HJ (1997) Gadolinium-ethoxybenzyl-DTPA as a hepatobiliary contrast agent for use in MR cholangiography: results of an in vivo phase-I clinical evaluation. *Eur Radiol* 7:126–132